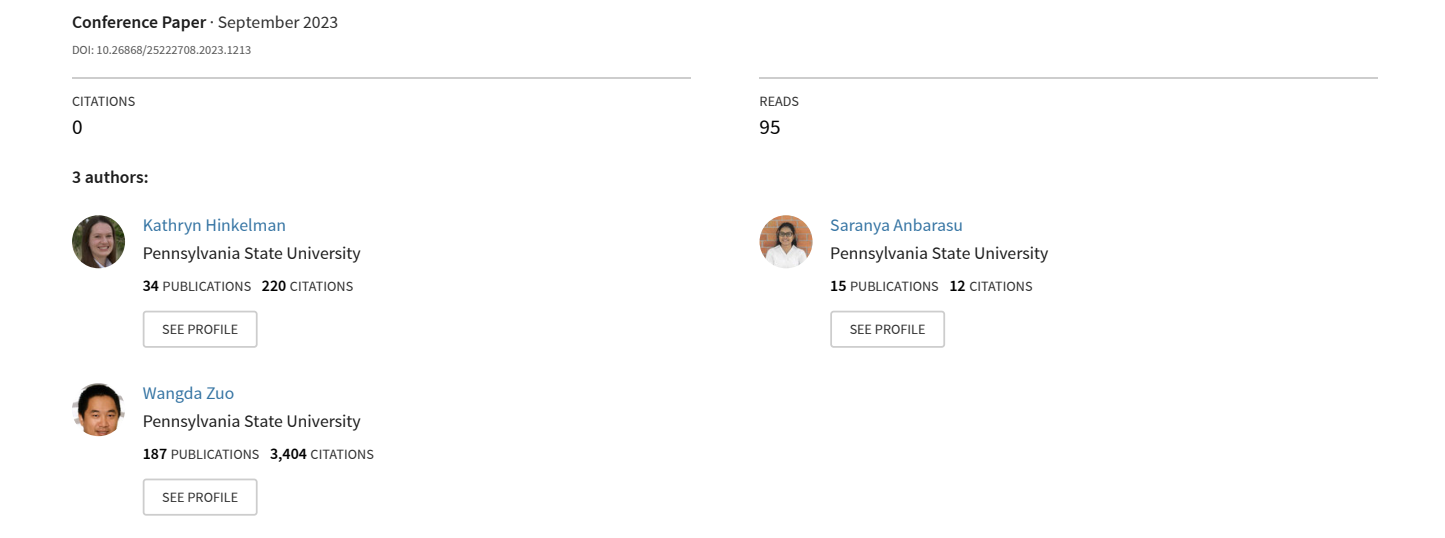
Ecological Network Analysis of Integrated Energy Systems with Modelica: A Novel Biomimetic Approach for Building Design and Operation



Ecological Network Analysis of Integrated Energy Systems with Modelica: A Novel Biomimetic Approach for Building Design and Operation

Kathryn Hinkelman¹, Saranya Anbarasu¹, Wangda Zuo^{1,2}
¹Pennsylvania State University, University Park, PA, USA
²National Renewable Energy Laboratory, Golden, CO, USA

Abstract

Ecological network analysis (ENA) combines modeling and analysis to study the structure, function, and organization of ecological food webs. Through biomimicry, ENA provides nature-inspired metrics for complex engineering systems. However, the major challenge is how to apply ENA to dynamic engineering system, such as buildings. To this end, we first formulate dynamic ENA on an exergy-basis in comprehensive mathematical models and implement the models in Modelica. Then, we validate our approach with a commonly referenced natural ecosystem. Using the Modelica models, we apply ENA for two building energy systems: an electrical system with renewable sources and a data center cooling system. Surprisingly, the results revealed that the data center conditioned air loop exchanged more exergy than the electrical energy supplied to the cooling system. For the electrical system, organizational metrics on a spectrum from highly redundant to highly efficient were in range with studied natural ecosystems, while the data center could benefit from higher redundancy. On a power basis, the analysis revealed large temporal variation in the electrical system's organization while the data center remained relatively constant. The paper concludes with future use cases of ENA for building design and operation.

Highlights

- The first to adopt ENA for building systems
- Adds complex network information beyond traditional efficiency-based metrics
- Provides a clear and comprehensive formulation for dynamic ENA
- Demonstrates that ENA can support the design and operation of integrated energy systems

Introduction

System integration is critical to attaining essential energy services with net-zero emissions (Davis et al., 2018). The same is true for building systems, where physical and operational integration

across multiple functional domains improves performance and comfort (Wetter, 2011). However, traditional efficiency-based metrics (i.e., input/output relationships) and optimization objectives (i.e., minimize costs, emissions, renewable curtailment) that still dominate today do not capture network complexity. To address the need for new system-of-systems (SOS) design and operational objectives, this work adopts biomimicry (ISO/TC 266, 2015) to develop biologically-inspired innovations. Many SOS features that create design and operational challenges for engineering systems are also present in natural ecosystems, which include complex dynamics, connectivity, agent heterogeneity, and others (Nielsen et al., 2020). Among the highly diverse and rapidly growing field of system-level biomimicry, ecological network analysis (ENA) is a leading approach that can meet this SOS need (Hinkelman et al., 2023).

In ENA, one analyzes exchanges of energy and/or materials through trophic levels of food webs to understand relationships between biodiversity and ecological stability (Coskun, 2019). Mathematically, ENA originates from information theory and graph theory, which is detailed in one of the seminal works by Ulanowicz (1986). Figure 1 depicts the standard ENA process from the physical ecosystem to the matrix model. The major steps are as follows. First, the ecological food web is mapped to a weighted digraph that represents the transfers of energy (or matter) with respect to participating agents (animals, plants, etc.) as edges f_{ij} , where i is the source and j is the sink. In Figure 1b, each agent represents a node, and electrical ground symbols represent losses. With graph theory, the weighted digraph can simply be represented as a matrix with elements f_{ij} , as shown in Figure 1c. Here, index 0 represents the inputs or outputs with respect to the external environment, and index n+1 represents the dissipation losses. From Figure 1c, ENA applies several whole-system metrics to quantify the organization of the network.

Since the pioneering works in the 1970's, ENA topics have spanned a wide range of biological, technical,

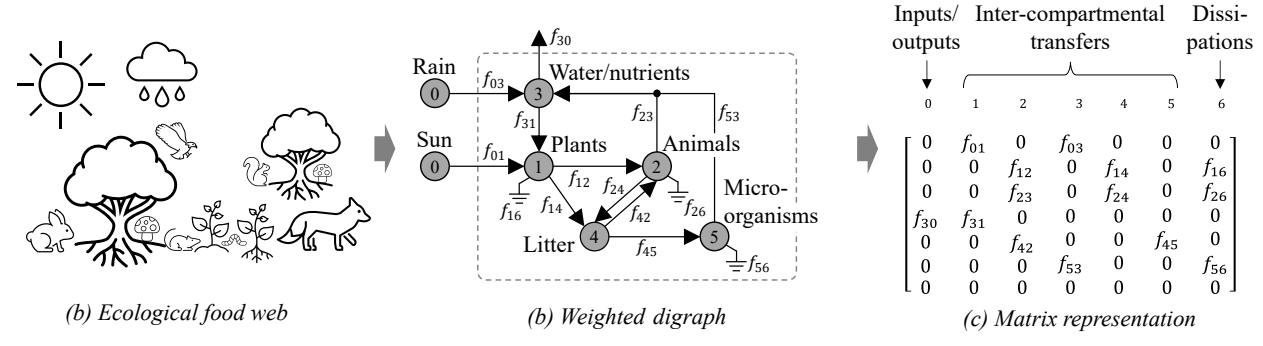


Figure 1: A typical ENA process from the (a) physical system to (b) network digraph to (c) matrix representation.

and social applications. Analysis of food web ecosystems have dominated literature, while energy and urban metabolism and wetland water systems have also benefited from ENA (Borrett et al., 2018). Leveraging biomimicry, engineering applications include industrial systems (Layton et al., 2016), manufacturing supply chains (Chatterjee and Layton, 2020), and cyber-physical power systems (Chatterjee et al., 2021). To date, all engineering studies focus on design with steady state ENA models. Although dynamic ENA (D-ENA) has been proposed in biological contexts (Coskun, 2019), there have yet to be any applications for dynamic engineering systems.

As such, it remains unclear how effective ENA is for such systems, which are dominant in real-world applications. To fill this gap, the purpose of this study is to develop and evaluate ENA for integrated building energy systems, which are complex dynamic engineering systems. First, we develop a comprehensive formulation for D-ENA in an engineering context. After validating the ENA implementation with a well-studied model, we then demonstrate the new analysis method for two case studies. As a novel method in the building's domain, we conclude with future use cases of ENA for both design and operation scenarios.

Methodology

Overview

This work addresses the need for new whole-systems analysis methods for integrated building energy systems. To solve this problem, we follow a *Biomimetics Technology Pull* approach from problem definition to prototyping (ISO/TC 266, 2015). In this work, food webs provide natural models to understand (1) how energy distributes through complex networks in ecosystems and (2) how trade-offs between *efficiency* and *redundancy* can improve an ecosystem's ability to rebound from disturbances (i.e., be *resilient*) and *sustain life* over time.

Similar to food webs, building energy systems are also complex networks, with several resiliency and sustainability aims being addressed by increasing renewable energy resources, expanding *prosumer* functionality, and incorporating energy diversity, among others.

With ENA, network organization metrics provide new information for engineering systems beyond the capabilities of traditional efficiency metrics that dominate today. While some preliminary works formulated D-ENA in biological contexts (Coskun, 2019), none are yet suitable for engineering applications. The primary contributions of this paper are the transfer of D-ENA methods from biology to engineering and the application of the new method for two case studies.

The following sections present D-ENA, which is suitable for dynamical, networked engineering systems. While this paper focuses on energy applications, this formulation could also be used for dynamic material networks (e.g., manufacturing/supply chains) or financial networks (e.g., corporate economics). For building energy systems, D-ENA is suitable for several scales, from equipment to complete grids.

Nomenclature

In biomimetics, it is common that the mathematical languages used in biology differ from those used in the engineering applications. As much as possible, we followed standard mathematical notation for the targeted building science audience, while maintaining variable assignments from ENA's biological origins. Like Coskun (2019) and Ulanowicz (1986), we define for n functional nodes: $X_i(t)$ is the total storage in node i with i = 1, ..., n at time t; $\dot{f}_{ij}(t, \cdot)$ is the nonnegative flow rate from node i to j at time t; $f_{i0}(t,\cdot)$ is the flow rate leaving the system boundary from node i at time t; $f_{0i}(t,\cdot)$ is the flow rate entering the system boundary into node i at time t; and $f_{i,n+1}(t,\cdot)$ is the dissipation rate (i.e., destruction rate) from node i at time t. Encompassing all flows, the total flow matrix is $\mathbf{F} = (f_{ij})$ with $0 \le i, j \le n+1$. Figure 2 visualizes this nomenclature.

In addition to the above assignments, we adopt several standard nomenclature from the engineering domain. Following thermofluid sciences, a dot above the variable indicates a flow rate (e.g., \dot{f} corresponds to power [W], while f corresponds to energy [J]). Thus, over simulation period $t \in [t_1, t_2)$, it follows that

$$f_{ij} = \int_{t_1}^{t_2} \dot{f}_{ij}(t,\cdot)dt.$$
 (1)

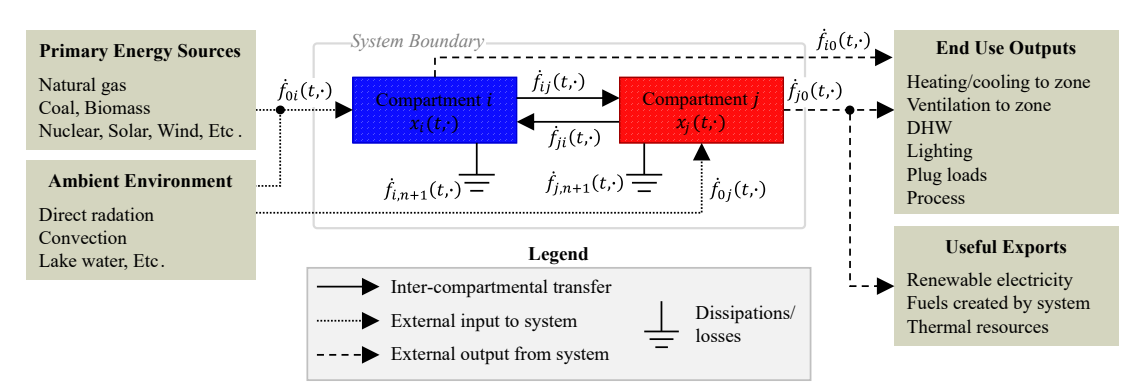


Figure 2: A generic full two-node network and system boundary for ENA in a building's context.

For multivariate functions, a center dot as in $f_i(\cdot)$ indicates that f is dependent on several other independent variables, which tend to vary across all i nodes.

Network Structure and Flows

Figure 2 depicts our suggested system boundary for ENA in a building's context, with flows to and from two nodes. We define the system boundary such that the total system efficiency η_s is

$$\eta_s = \frac{\sum f_{0i}}{\sum f_{i0}} = \frac{\text{end use outputs+useful exports}}{\text{primary energy+environment inputs}}.$$
 (2)

Examples of end use exports, useful exports (to other heterogeneous systems), and primary energy/environmental inputs are given in Figure 2. In this work, we adopt the definition for primary energy by Standard 105 (ANSI and ASHRAE, 2014), which includes site energy plus all energy consumed/lost from the point of extraction of primary energy forms (e.g., coal, natural gas, nuclear fuel). The resolution of nodal boundaries can be selected based on the modeler's needs and data availability. For example, a district energy simulation may lump the HVAC system for each building as one node, while a single building simulation may represent each equipment as one node.

For any node i, the governing system of equations for D-ENA is

$$\frac{dX_i}{dt} = \sum_{j=0}^{n+1} \dot{f}_{ji}(t,\cdot) - \sum_{j=0}^{n+1} \dot{f}_{ij}(t,\cdot) \tag{3}$$
inward flow rates outward flow rates
$$X_i(t_0) = X_{i,0}, \ \forall \ i = 1, ..., n,$$

where X_i is the useful energy (i.e., exergy) stored in node i at time t; the first summation represents all inward flow rates to i; and the second summation represents all outward flow rates from i. For the complete system, the balance is

$$\sum_{i=1}^{n} \frac{dX_i}{dt} = \sum_{i=0}^{n} \left[\dot{f}_{0i}(t,\cdot) - \dot{f}_{i0}(t,\cdot) - \dot{f}_{i,n+1}(t,\cdot) \right]. \tag{4}$$

Further explanation on the need for exergy analysis is given under *Implementation*.

ENA Metrics

Beyond structure and flows, ENA leverages information theory to quantify the organization of conserved properties in complex networks. In standard ENA, the foundational metrics are the *capacity* for system development c, the *ascendancy* a, and the *overhead* ϕ . Defined in Ulanowicz (1986), these are

$$c = -\sum_{i=0}^{n+1} \sum_{j=0}^{n+1} \frac{f_{ij}}{\Psi} \ln \left(\frac{f_{ij}}{\Psi} \right), \tag{5}$$

$$a = \sum_{i=0}^{n+1} \sum_{j=0}^{n+1} \frac{f_{ij}}{\Psi} \ln \left(\frac{\Psi f_{ij}}{\tau_{out,i} \tau_{in,j}} \right), \text{ and }$$
 (6)

$$\phi = -\sum_{i=0}^{n+1} \sum_{j=0}^{n+1} \frac{f_{ij}}{\Psi} \ln \left(\frac{f_{ij}^2}{\tau_{out,i} \tau_{in,j}} \right), \tag{7}$$

where Ψ represents the total system throughput as

$$\Psi = \sum_{i=0}^{n+1} \sum_{j=0}^{n+1} f_{ij}, \tag{8}$$

and $\tau_{in,i}$ and $\tau_{out,i}$ represent the total inward and outward throughflows at node i as

$$\tau_{in,i} = \sum_{j=0}^{n+1} f_{ji} \quad \text{and}$$
 (9)

$$\tau_{out,i} = \sum_{j=0}^{n+1} f_{ij}.$$
 (10)

A frequently adopted metric, degree of system order $\alpha = a/c$ indicates the organization (or the lack of flow diversity) in a networked system. By definition, the decomposition of capacity is $c = a + \phi$. Thus, it is guaranteed that $\alpha \in [0,1]$ because $a \leq c$ and $c, a, \phi \geq 0$. As unitless ratio from 0 (high redundancy/diversity) to 1 (high efficiency/low diversity), it is an effective metric to compare order across different systems (Ulanowicz, 2004) and for evaluating resiliency (Chatterjee and Layton, 2020). With this basis, previous ENA literature identified a window of vitality for biological ecosystems that clustered in

 $25\% \leq \alpha \leq 53\%$ (Chatterjee et al., 2021). Previous ENA studies show that ecosystems falling in this range are at an optimal balance between redundancy and efficiency, and that this range can be considered a desirable level of organization for sustainable development (Fath, 2015).

Lastly, Finn's Cycling Index FCI "accounts for the percentage of all [flows] that is generated by cycling" (Allesina and Ulanowicz, 2004). Mathematically, FCI is

$$FCI = \sum_{i=1}^{n} \frac{\tau_{in,i}}{\Psi} \left(\frac{l_{ii} - 1}{l_{ii}} \right), \tag{11}$$

where l_{ii} is the *i*th entry along the diagonal of the Leontief matrix $\mathbf{L} = [\mathbf{I} - \mathbf{G}]^{-1}$, with identify matrix **I** and fractional inflow matrix $\mathbf{G} = (f_{ij}/\tau_{in.i})$. For 100 ecosystem models, Borrett and Lau (2014) found that FCI ranged from 0–98% with a mean of 38%. Layton et al. (2016) found that maximizing FCI as a biologically inspired optimization objective for industrial supply chains correlates strongly with traditional objective functions based on emissions and costs.

Equations (5)-(11) are standard ENA. However, there are a few notable differences between this and previous ENA works. First, we adopt Ψ for total system throughput instead of the commonly-used T, because T is used for temperature in thermofluid sciences. Second, extrinsic ENA metrics are often used $(C, A, \text{ and } \Phi)$, where $A = a\Psi$ encompasses both the "total activity" through Ψ and the "organization by which component processes are linked" through a (Ulanowicz, 2004). Instead, we adopt the intrinsic versions $(c, a, and \phi)$ to maintain equivalence with information theory and allow the results to be extensible to other system types and sizes, similar to Rutledge et al. (1976). Third, ENA metrics allow for several logarithmic bases to be appropriate. While $\log_2(\cdot)$ is often selected (such as in Ulanowicz (1986), where the units for a, c, and ϕ are "bits"), we keep consistency with data science and engineering practices by adopting $ln(\cdot)$ (base e with units of "nats"). Finally, we formulate ENA for dynamical systems, which, to our knowledge, is novel for engineering applications. As such, we replace constant the f_{ij} terms with dynamically-calculated, multivariate functions using (1). This extends Coskun (2019), where network structure and flows were defined dynamically, but ENA metrics were excluded. Further, to understand ENA metrics dynamically, we newly define them on a power-basis (indicated with subscript p). For example, power-based ascendancy a_n is

$$a_p = \sum_{i=0}^{n+1} \sum_{j=0}^{n+1} \frac{\dot{f}_{ij}}{\Psi_p} \ln\left(\frac{\Psi_p \dot{f}_{ij}}{\dot{\tau}_{out,i} \dot{\tau}_{in,j}}\right),$$
 (12)

where $\Psi_p = \sum_{ij} \dot{f}_{ij}$ is the total system throughput power. Other metrics $(c_p, \phi_p, \alpha_p, \text{ etc.})$ follow a similar approach. Further, we advance Coskun's work

from ecological systems with low-order ordinary differential equations to engineering systems with stiff, hybrid differential algebraic equations. As such, this work is the first to provide a pathway for applying D-ENA for numerous complex system models across the engineering sciences and real-world practices.

Implementation

By convention, ENA represents all flow rates f_{ij} in absolute terms. This is in contrast to standard energy analysis of thermofluid systems, where control volume analysis involves relative changes in fluid's enthlapy across system boundaries. To allow meaningful comparisons across multiple energy types (i.e., electricity to hot water), we formulate all flow rates \dot{f}_{ij} on an exergy basis. For the exergy dead state, this work uses the current outdoor air temperature. This provides the most meaningful formulation because (1) exergy is concerned with the portion of energy that has the potential to do work with respect to the surroundings, and (2) operating temperatures for building systems are frequently near ambient, and both the operating and ambient temperatures vary with time.

Unique among ENA literature, this work adopts a generic balance for the exergy X in node i as

$$\frac{dX_i}{dt} = \sum_{k} \left(1 - \frac{T_0}{T_k}\right) \dot{Q}_k \tag{13a}$$

$$-\left(\dot{W} - p_0 \frac{dV_{cv}}{dt}\right) \tag{13b}$$

$$+ \sum_{j} \dot{m}_{j} |(h_{j} - h_{0}) - T_{0} (s_{j} - s_{0})|$$

$$- \dot{X}_{f} + \dot{X}_{ke} + \dot{X}_{pe} - \dot{X}_{d},$$
(13d)

$$-\dot{X}_f + \dot{X}_{ke} + \dot{X}_{pe} - \dot{X}_d,$$
 (13d)

where the right hand terms in (13) represent the heat transfer (13a); the useful and boundary work (13b); the thermofluid inflow and outflow (13c); and the chemical exergy of fuels, kinetic and potential energy, and exergy destruction (13d). Temperature is T, pressure is p, volume is V, heat flow rate is \dot{Q} , work rate is \dot{W} , mass flow rate is \dot{m} , specific enthlapy is h, and specific entropy is s. For subscripts, 0 is the dead state, cv is the control volume, f is chemical fuel, ke is kinetic energy, pe is potential energy, and d is destruction. In (13c), we formulate the thermofluid exergy with absolute values to maintain the same sign direction as the mass flow rate regardless of whether the fluid is cold or hot relative to the dead state (Jansen and Woudstra, 2010). This ensures that all $f_{ij} \geq 0$, consistent with ENA standards and the standard conceptualization that all useful work is positive. Exergy analysis is a well-established field by itself; for a building's context, interested readers can find more information in Evola et al. (2018).

To enable ENA of complex, dynamical system models for the first time, we implement D-ENA in Modelica, an equation-based and object-oriented modeling language. There are several benefits to this, including the support of both causal and acausal modeling and the availability of several numerical solvers. Examples of Modelica-based modeling related to this work are available in the Modelica Buildings Library (Wetter et al., 2014) and the Biomimetic Integrated Community Energy and Power Systems (BICEPS) Library (Hinkelman and Zuo, 2022).

Validation

To validate our Modelica formulation, we implement a commonly-cited model from ecology: Cone Springs (Tilly, 1968). This cold spring ecosystem in Iowa, U.S. has often been studied in ecology because of its small size, isolated location, and relatively constant physical and chemical conditions (Tilly, 1968). Depicted in Figure 3, the Cone Spring ENA model is steady state with five nodes (plants, detritus, bacteria, carnivores, and detritivores).

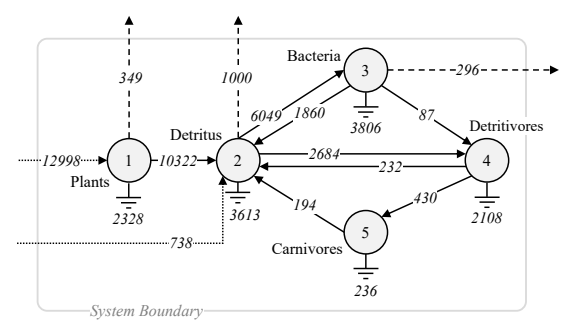


Figure 3: Energy exchange network (Wh/m²/y) for Cone Springs. Solid edges represent inter-nodal exchanges; dotted edges represent external inputs; dashed edges represent external outputs; and ground symbols represent dissipations.

The network structure and flows in Figure 3 (without dissipations) are inputs for the Modelica model. Then, we run the steady state simulation to calculate dissipations and all ENA metrics. From this simulation, the calculated Ψ was 49.3 kWh/m²/y; a was 0.926 nats; c was 2.22 nats; ϕ was 1.29 nats; α was 41.8%, and FCI was 6.60%. All values obtained for final ENA metrics and intermediate calculations (i.e, elements of \mathbf{L}) are consistent with previous works (Ulanowicz, 1986, 2004).

Case Studies

We select two models in the Modelica Buildings Library (Wetter et al., 2014) v9.0.0 for demonstration: (1) a grid-tied electrical system with renewable sources and (2) a data center cooling system with integrated chillers and waterside economizer (WSE). Both models are extended with D-ENA and simulated with CVODE solver for one year. In this section, we present the case study models and simulation results.

Renewable Sources Model

The RenewableSources model in the Buildings Library's Electrical subpackage demonstrates the im-

pact of renewable sources on the electric grid. This model contains seven loads, seven photovoltaic (PV) arrays, one wind turbine, an electric grid connection, and eight power lines. The PV and wind turbine sizing result in load cover factors between 40 and 110%. From the system model, we first map all equipment to nodes and draw the directed network graph. This network graph is shown under Results in Figure 5a. Then, we determine all functions $f_{ij}(t,\cdot)$ and formulate F, from which all following ENA metrics are calculated as post-processing blocks. Figure 4 shows the final model, which includes the base RenewableSources system model; ten ENA node blocks (circles overlaid on model equipment); three primary inputs; one end use output; and ENA post-processing for ENA below the system. The network description blocks store all f_{ij} elements as a total flow matrix F, from which all following metrics are causally calculated. Consistent with Peterson et al. (2015), we assume a source energy conversion factor of 3.15 for imported electricity and exported renewable energy. For a primary energy basis, wind and PV electricity production are considered 100% per ANSI and ASHRAE (2014). Meanwhile, we assume 90% DCto-AC conversion efficiencies.

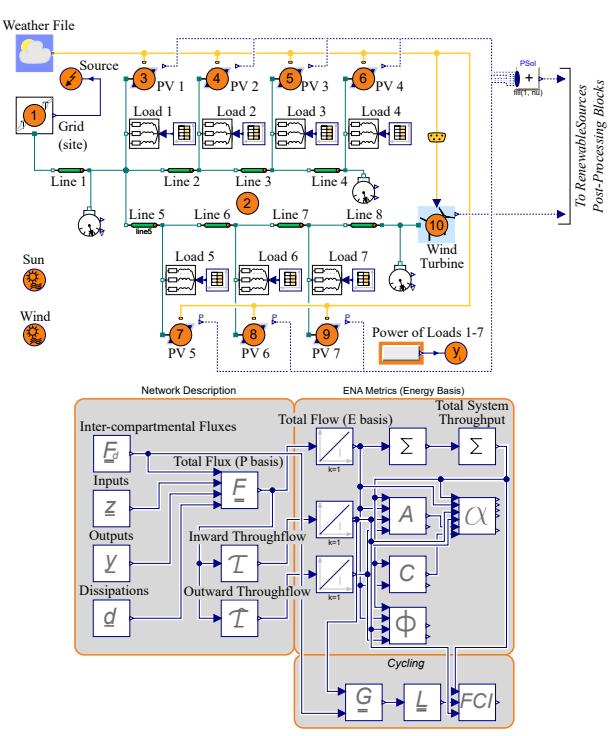


Figure 4: Modelica diagram of the RenewableSources model with ENA nodes and post-processing calculation blocks indicated with orange.

This model involves dynamic flows and steady energy balances, since energy storage is negligible for these electrical components. As an example, the balance (3) for node 2 (power lines 1-7) is

$$0 = P_{ele} + P_{win} + \sum P_{pv} - \sum P_{loa} - P_{loss}, \quad (14)$$

where P is power and subscripts ele is the electric grid, win is the wind turbine, pv is photovoltaic, loa is the end use loads, and loss is losses in the wires. For electrical systems, note that (14) represents both the energy and exergy balance.

Data Center Model

For a thermofluid example, we adopt the data center cooling system IntegratedPrimaryLoadSideEconomizer from the Applications/DataCenters package of the Buildings Library. To cool the data center server room, the system contains two chillers, an integrated WSE, two cooling towers, and an air handling unit (AHU) with humidification. Similar to Figure 4, we extend the existing Buildings Library model with ENA nodes and post-processing blocks. This system contains four nodes (cooling tower subsystem, chiller/WSE subsystem, AHU, and electric grid); one primary energy source (source energies from the electric grid); and one end use output (server room). The network graph for this system is shown under Results in Figure 5b.

Because this system contains both thermofluid and electrical energy flows, we model the network with exergy balances. We assume the cooling tower and chiller/WSE subsystems have dynamic exergy balances, while the AHU and electrical grid are steady with negligible storage. For an example, exergy in node 3 (chiller/WSE subsystem) is

$$\frac{dX_3}{dt} = \dot{f}_{13} + \dot{f}_{23} + \dot{f}_{43} - \dot{f}_{32} - \dot{f}_{34} - \dot{f}_{35} \qquad (15)$$

$$= P_{ch} + P_{chwp} - \dot{X}_{d3}$$

$$+ \dot{m}_{cws} |h_{cws} - h_0 - T_0(s_{cws} - s_0)|$$

$$+ \dot{m}_{chwr} |h_{chwr} - h_0 - T_0(s_{chwr} - s_0)|$$

$$- \dot{m}_{cwr} |h_{cwr} - h_0 - T_0(s_{cwr} - s_0)|$$

$$- \dot{m}_{chws} |h_{chws} - h_0 - T_0(s_{chws} - s_0)|$$
and
$$X_3 = \sum_{i=1}^4 m_{ch,i} |h_{ch,i} - h_0 - T_0(s_{ch,i} - s_0)|, \quad (16)$$

where subscripts ch is chillers, chwp is chilled water pumps, chws is chilled water supply, chwr is chilled water return, cws is condenser water supply, and cwr is condenser water return. Subscript 0 represents the dead state, taken as water at thermodynamic equilibrium with the surrounding air (atmospheric pressure and outdoor air drybulb temperature). When air is present (e.g., in the AHU), we use dynamic mass fractions of water vapor for both the outdoor air (dead state) and conditioned air. For the chiller/WSE, (15) is the dynamic exergy balance, while (16) is the exergy stored in the chiller water volumes at time t. Together, the solver calculates the time-varying exergy destruction (i.e., dissipation) \dot{X}_{d3} .

Results

Table 1 presents the ENA metrics for both case studies over annual simulations. The total system efficien-

cies η_s (2) for the renewable sources and data center models are 42.4% and 83.1%, respectively. While a is similar for both systems, renewable sources has higher c and ϕ . This results in an renewable sources α within the window of vitality, while the data center α indicates that the system could benefit from higher redundancy. For FCI, both systems exhibit low degrees of cycling.

Table 1: ENA metrics for the two case study systems.

Metric	Renewable	Data	Units
	Sources	Center	Units
Ψ	546	29100	MWh/y
a	0.919	0.924	nats
c	2.56	1.48	nats
ϕ	1.64	0.561	nats
α	35.9	62.2	%
FCI	2.63	0.581	%

Figure 5 shows the exergy exchanges throughout each network as weighted digraphs. newable sources, the path source energies $\rightarrow electrical$ $grid \rightarrow dissipations$ dominates all possible paths. For the data center, the simple cycle between the AHU and server dominates. This latter result is surprising because electricity is the highest quality energy, and thus we often expect electrical exergy to dominate. Two findings are important to understand this result. First, the relative change in exergy between supply and return air streams is smaller than the electrical exergy flows, which follows expectations. Second, the absolute-flow perspective with ENA reveals that the air cooling the data center server room operates as a high exergy loop. Compared to the water loops in Figure 5b (which are low exergy), the conditioned air loop is high exergy because (1) the supply air mass flow rate \dot{m}_{sa} is 7.9 times higher than \dot{m}_{chws} on average, (2) the mass fraction of water in the conditioned air is 3.4 times higher than the average outdoor air mass fraction due to humidification in the AHU, and (3) $T_{ra} > T_{sa} > T_{chws}$ and often $T_{ra}, T_{sa} \gg T_0$, where T_{ra} is the return air temperature from the server room. Contrary to studying relative energy/exergy flows, as typically done, this absolute exergy network-based perspective reveals opportunities to capture waste heat and/or switch to a liquid cooling technology for server equipment.

Figure 6 presents the evolution of ENA metrics on a power-basis. Across all power-based metrics, the data center exhibits relatively low variability with respect to time. Mean and standard deviations for the data center $a_p,\ c_p,\ \phi_p,$ and α_p are 0.92 ± 0.033 nats, 1.6 ± 0.19 nats, 0.69 ± 0.18 nats, and $58\pm5.5\%$, respectively. In contrast, the renewable sources model has high daily variability in multiple power-based ENA metrics. Mean and standard deviations for renewable sources $a_p,\ c_p,\ \phi_p,$ and α_p are 1.0 ± 0.055 nats, 2.0 ± 0.60 nats, 0.92 ± 0.56 nats, and $58\pm14\%$, respectively.

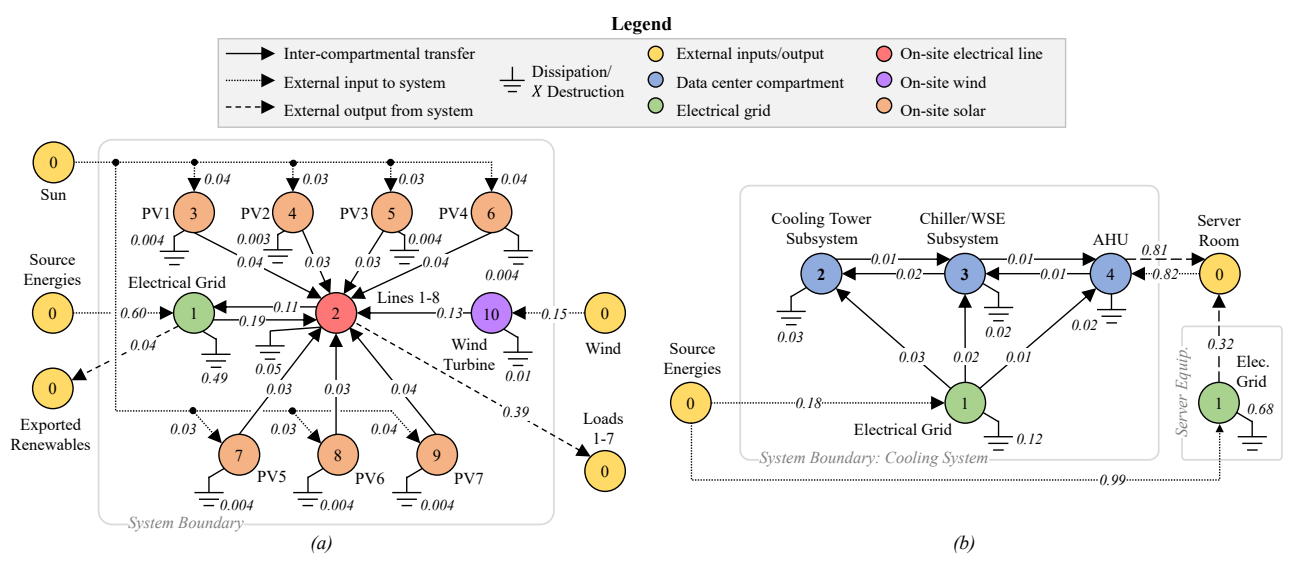


Figure 5: Normalized annual exercy (J/J) for the (a) renewable sources and (b) data center cooling systems, normalized by the sum of primary inputs such that $\sum f_{0i} = 1$. In (b), the out-of-scope server equipment system is shown in parallel to the cooling system because it largely influences the results.

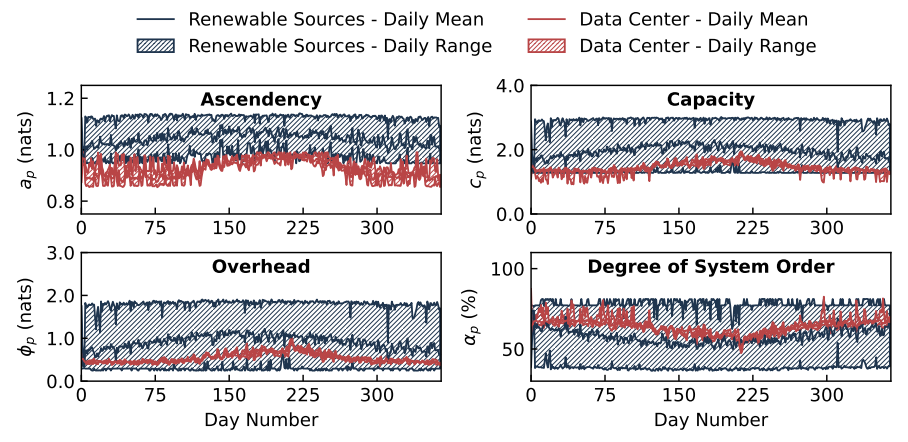


Figure 6: Evolution of power-based ENA metrics for Renewable Sources and Data Center models.

tively. Changes in c_p and ϕ_p are directly proportional to $\sum P_{pv}$, while α_p is inversely proportional to $\sum P_{pv}$. This follows expectations, where higher power diversity resulted in lower degree of system order.

Conclusion

While efficiency indicates the ratio of outputs to inputs, ENA gives an indication of network complexity and quantifies organization in several ways. This paper is the first to demonstrate D-ENA for engineering applications, and the first to apply ENA for building systems. After formulating D-ENA in Modelica, the electrical (renewable sources) model exhibited similar performance in the efficiency-to-redundancy trade space as sustainable natural ecosystems, while the thermofluid (data center) system results suggested that higher redundancy may be desired. Meanwhile, low degrees of cycling were present in both systems, indicating an opportunity to improve cycling through waste recovery or other recycling technologies for fu-

ture integrated and resilient energy systems.

As a pioneering study on D-ENA, applying this method for design or operation of engineering systems remain unexplored. In a design context, future studies may leverage network information to select technology investments (e.g., add PV or storage, switch to liquid cooling). For operational purposes, it would be interesting to evaluate the benefits of α and FCI for determining system response strategies under stress. With the transition of energy and building systems towards dynamic, interconnected, zero-emission systems, innovative methods such as D-ENA may provide invaluable information.

Acknowledgment

The authors thank Michael Wetter and the reviewers for their constructive comments, which helped us to improve the quality of the manuscript. This research was supported in part by an appointment with the IBUILD Graduate Student Research Pro-

gram sponsored by the U.S. Department of Energy (DOE), Office of Energy Efficiency and Renewable Energy, and Building Technologies Office. This program is managed by Oak Ridge National Laboratory (ORNL). This program is administered by the Oak Ridge Institute for Science and Education (ORISE) for the DOE. ORISE is managed by ORAU under DOE contract number DESC0014664. All opinions expressed in this paper are the author's and do not necessarily reflect the policies and views of DOE, ORNL, ORAU, or ORISE. This material is also based upon work supported by the National Science Foundation under Award No. 2025459. Lastly, this work emerged from the IBPSA Project 1, an international project conducted under the umbrella of the International Building Performance Simulation Association (IBPSA). Project 1 will develop and demonstrate a BIM/GIS and Modelica Framework for building and community energy system design and operation.

References

- Allesina, S. and R. E. Ulanowicz (2004). Cycling in ecological networks: Finn's index revisited. Computational Biology and Chemistry 28(3), 227–233.
- ANSI and ASHRAE (2014). Standard methods of determining, expressing, and comparing building energy performance and greenhouse gas emissions. *Standard* 105-2014.
- Borrett, S. R. and M. K. Lau (2014). enaR: An R package for Ecosystem Network Analysis. *Methods in Ecology and Evolution* 5(11), 1206–1213.
- Borrett, S. R., L. Sheble, J. Moody, and E. C. Anway (2018). Bibliometric review of ecological network analysis: 2010–2016. *Ecological Modelling* 382, 63–82.
- Chatterjee, A., H. Huang, K. R. Davis, and A. Layton (2021). A Multigraph Modeling Approach to Enable Ecological Network Analysis of Cyber Physical Power Networks. In *IEEE International Confer*ence on Communications, Control, and Computing Technologies for Smart Grids, pp. 239–244.
- Chatterjee, A. and A. Layton (2020). Mimicking nature for resilient resource and infrastructure network design. *Reliability Engineering and System Safety* 204, 107142 Contents.
- Coskun, H. (2019). Dynamic ecological system analysis: A holistic analysis of compartmental systems. Heliyon 5(9), e02347.
- Davis, S. J., N. S. Lewis, M. Shaner, S. Aggarwal, D. Arent, and I. L. Azevedo et al. (2018). Net-zero emissions energy systems. Science 360 (6396).
- Evola, G., V. Costanzo, and L. Marletta (2018). Exergy analysis of energy systems in buildings. Buildings~8(12).

- Fath, B. D. (2015). Quantifying economic and ecological sustainability. Ocean and Coastal Management 108, 13–19.
- Hinkelman, K., Y. Yang, and W. Zuo (2023). Design methodologies and engineering applications for ecosystem biomimicry: An interdisciplinary review spanning cyber, physical, and cyber-physical systems. *Bioinspiration & Biomimetics* 18(2), 021001.
- Hinkelman, K. and W. Zuo (2022). BICEPS Modelica library (v0.1.0). https://sites.psu.edu/sbslab/tools/biceps-library.
- ISO/TC 266 (2015). Biomimetics Terminology, concepts and methodology (1st ed.), Volume 18458. ISO.
- Jansen, S. and N. Woudstra (2010). Understanding the exergy of cold: Theory and practical examples. *International Journal of Exergy* 7(6), 693–713.
- Layton, A., B. Bras, and M. Weissburg (2016). Designing Industrial Networks Using Ecological Food Web Metrics. Environmental Science and Technology 50(20), 11243–11252.
- Nielsen, S. N., B. D. Fath, S. Bastianoni, J. C. Marques, F. Müller, B. C. Patten, R. E. Ulanowicz, S. E. Jørgensen, and E. Tiezzi (2020). A New Ecology: Systems Perspective (2nd ed.).
- Peterson, K., P. Torcellini, and R. Grant (2015). A Common Definition for Zero Energy Buildings. U.S. DOE Report.
- Rutledge, R. W., B. L. Basore, and R. J. Mulholland (1976). Ecological stability: An information theory viewpoint. *Journal of Theoretical Biology* 57(2), 355–371.
- Tilly, L. J. (1968). The Structure and Dynamics of Cone Spring. *Ecological Monographs* 38(2), 169–197.
- Ulanowicz, R. E. (1986). Growth and Development: Ecosystems Phenomenology. New York: Springer-Verlag.
- Ulanowicz, R. E. (2004). Quantitative methods for ecological network analysis. *Computational Biology* and Chemistry 28, 321–339.
- Wetter, M. (2011). A View on Future Building System Modeling and Simulation. In J. L. M. Hensen and R. Lamberts (Eds), *Building Perfor*mance Simulation for Design and Operation, Chapter 17. Routledge, UK: Taylor & Francis Group.
- Wetter, M., W. Zuo, T. S. Nouidui, and X. Pang (2014). Modelica Buildings Library. *Journal of Building Performance Simulation* 7(4), 253–270.